Contrib Mineral Petrol (1990) 106:100–109

Contributions to Mineralogy and Petrology

Petrogenesis of cordierite-orthoamphibole assemblages from the Springton region, South Australia

Jo Arnold and Michael Sandiford

Department of Geology and Geophysics, University of Adelaide, GPO Box 498, Adelaide, South Australia

Received March 9, 1990 / Accepted June 20, 1990

Abstract. Textural evidence for the partial breakdown of staurolite-biotite and andalusite-biotite assemblages to cordierite-orthoamphibole implies high temperature metasomatic depletion of K_2O in semi-pelitic rocks from Springton, South Australia. The origin of the reaction textures is discussed with reference to μK_2O-T diagrams derived from the topologically equivalent μK_2O–(-μH_2O) diagram showing both discontinuous and Fe–Mg continuous reactions. The involvement of fluids in the metasomatic process is implied by the scale of K_2O removal and suggests that the outcrop pattern of cordierite-gedrite rocks reflects, at least in part, a heterogeneous distribution of advecting fluids in the metamorphic pile at high temperatures.

Introduction

Cordierite-orthoamphibole rocks have attracted considerable interest because of their unusual bulk compositions (e.g. Chinner and Fox 1974), and the complex textures they often display (e.g. Robinson and Jaffe 1969; Harley 1985; Schumacher and Robinson 1987; Baker et al. 1987). Their low proportions of K_2O and/or CaO and high Na_2O/K_2O ratios contrast with more typical sedimentary or igneous rocks with similar Al_2O_3 contents. These unusual chemical characteristics have been explained in a number of ways (e.g. Hudson and Harte 1985; Spear and Schumacher 1982) which fall into two main groups; (1) the isochemical metamorphism of rocks with unusual compositions and (2) the synmetamorphic chemical modification (or metasomatism) of rocks with more typical compositions. The common association of cordierite-orthoamphibole rocks with metamorphosed exhalative sulphide deposits (e.g. Chinner and Fox 1974) and the similarity of their bulk composition to that of chlorite-quartz rocks suggest that many cordierite-orthoamphibole rocks may represent metamorphosed hydrothermal alteration products. In contrast, Sandiford et al. (1990) suggested that cordierite-gedrite rocks in the Springton region of the Mount Lofty Ranges, South Australia, preserve evidence of high temperature metasomatic depletion of K_2O from semi-pelitic and pelitic schists. This interpretation has important implications for the distribution and behaviour of fluids in metamorphic terrains which in turn is critical to the evaluation of the way in which heat and mass are transported within the metamorphic pile. In this paper we investigate the theoretical constraints on the genesis of cordierite-orthoamphibole rocks by high temperature metasomatism of semi-pelitic rocks in order to provide the basis for the interpretation of the origin of cordierite-gedrite rocks near Springton. Finally we briefly consider the implications of cordierite-orthoamphibole genesis for the behaviour of fluids during regional metamorphism in the Springton region.

Theoretical considerations

The connection between cordierite-orthoamphibole rocks and semi-pelites consisting of quartz + biotite + plagioclase (± staurolite, cordierite, aluminosilicate, garnet) is easily demonstrated with an AKFm plot (Fig. 1). At appropriate grades removal of K_2O from a semi-pelite drives its bulk composition from the biotite (± staurolite, cordierite, aluminosilicate) field towards the A-Fm boundary, stabilizing cordierite-orthoamphibole or cordierite-garnet, depending on the relative stability of orthoamphibole and garnet. In order to deal with the prograde metamorphism of rocks in which the K_2O-content may vary with time, it is useful to consider the

Offprint requests to: J. Arnold

[1] Mineral abbreviations used in text and figures: ab, albite; alm, almandine; als, aluminosilicate; and, andalusite; anth, anthophyllite; bt, biotite; cd, cordierite; fe-bt, Fe-rich biotite; fe-cd Fe-rich cordierite; fe-oa, Fe-rich orthoamphibole; fe-st, Fe-staurolite; gt, garnet; ksp, potassium feldspar; ky, kyanite; mg-cd, Mg-rich cordierite; mg-oa, Mg-rich orthoamphibole; mg-st, Mg-rich staurolite; mu, muscovite; oa, orthoamphibole; phl, phlogopite; plag, plagioclase; py, pyrope; sill, sillimanite; st, staurolite; v, vapour

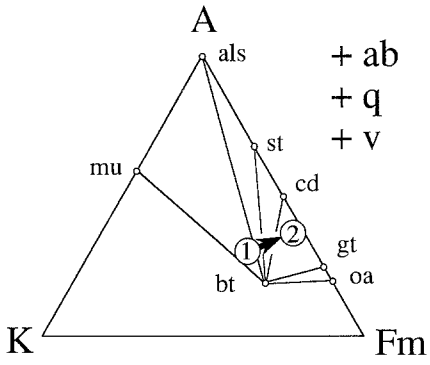

Fig. 1. AKFm diagram showing bulk composition of pelitic and semi-pelitic rocks shown by *region 1*, and cordierte-orthoamphibole rocks (*region 2*). Apices are A: Al_2O_3, K: K_2O, Fm: FeO + MgO, projected from albite, quartz and vapour (in excess). Depletion of K_2O in pelites produces cordierite-orthoamphibole (or, at appropriate grades and X_{Fe}, cordierite-garnet) assemblages at the expense of the pelite/semi-pelite assemblage

chemical potential of K_2O (μK_2O) with changing physical conditions (e.g. pressure and temperature) of metamorphism. An effective way to represent this is to use a μK_2O-T or μK_2O-P diagram. This section outlines the basis for the construction of such diagrams appropriate to mineral assemblages common in aluminous cordierite-orthoamphibole rocks from a wide variety of locations.

Mineralogy of cordierite-orthoamphibole rocks

Cordierite-orthoamphibole rocks contain a diverse suite of minerals, including sapphirine, corundum or quartz, spinel, ilmenite, rutile, plagioclase, chlorite, aluminosilicate, staurolite, biotite and garnet (e.g. Robinson and Jaffe 1969; Sharma and MacRae 1981; Baker et al. 1987; Schumacher and Robinson 1987). In this paper we consider semi-pelitic compositions, which are invariably saturated in silica (i.e. with free quartz), which therefore precludes the existence of sapphirine, spinel and corundum. In most cases chlorite occurs as a late stage alteration product – rarely, if ever, in equilibrium with the cordierite-orthoamphibole assemblage. Ilmenite and/or rutile are stabilized only when there is a significant amount of TiO_2 in the rock, as is the case for most semi-pelites. At low pressures (i.e. andalusite-sillimanite facies metamorphism) ilmenite is typically a saturating phase, while at higher pressures (kyanite-sillimanite facies) rutile is more common. Although the Ti-phases have been disregarded for this study, all diagrams may easily be extended into the Ti-system by incorporating either rutile or ilmenite into reactions in addition to Ti-biotite. The remaining phases considered here, therefore, are quartz, plagioclase, aluminosilicate, staurolite, biotite, garnet, cordierite and orthoamphibole. The relative X_{Fe} (FeO/(FeO + MgO)) of these minerals generally decreases in the order gt > st > oa > bt > cd, as shown in Fig. 2b.

FMASH and NFMASH

As a starting point, consider the K_2O-absent system, $FeO-MgO-Al_2O_3-SiO_2-H_2O$ (FMASH), involving the phases quartz, aluminosilicate, staurolite, garnet, cordierite, orthoamphibole and vapour; see Fig. 3. The pressure-temperature stability relations for this $(n+2)$ system, which necessarily involves only one invariant point, termed Ip_1, have been discussed by a number of workers (e.g. Hudson and Harte 1985; Baker et al. 1987). Ip_1 occurs at approximately 650° C and 4.5 kbar (Fig. 3). For rocks with quartz and vapour in excess, five univariant reactions diverge from Ip_1, (st), (gt), (cd) to higher pressures and (als), (oa) to lower pressures. Each of the five univariants terminate in a FASH or MASH invariant point, the position of which has been calculated using "THERMOCALC" (Powell and Holland 1988), assuming Al- and Na-free anthophyllite (in nature it is probable that these limiting end-member invariants will be metastable with respect to assemblages involving other phases such as chlorite and/or orthopyroxene).

Since naturally occurring orthoamphiboles are typically sodic, the addition of Na_2O will expand the stability field of orthoamphibole with respect to other Fe–Mg phases. Semi-pelites are typically sufficiently saturated in Na_2O to stabilize Na-rich plagioclase. Thus, Fig. 3 can be viewed schematically as the NFMASH system projected from quartz, vapour and albite. The position

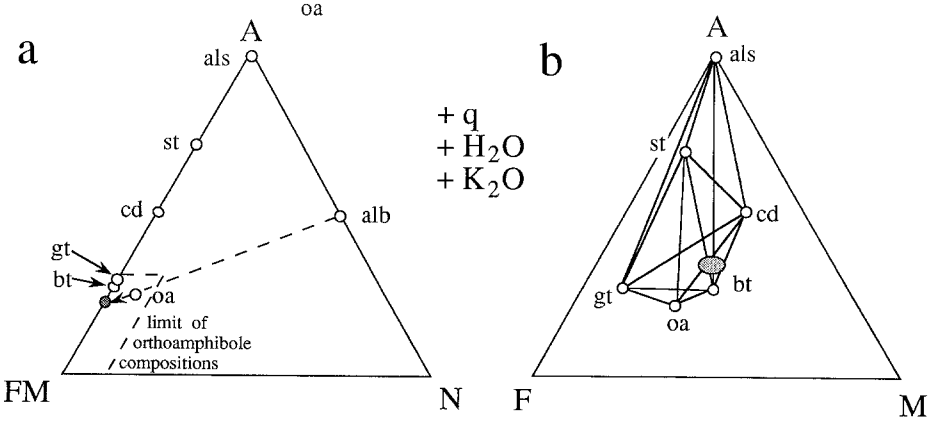

Fig. 2. a ANFm diagram showing the projection of orthoamphibole from albite onto the AFM plane of **b**. Apices are *A*: Al_2O_3, *N*: Na_2O; *FM*: FeO + MgO, projected from K_2O (considered to be perfectly mobile), vapour and quartz (in excess). **b** AFM diagram showing composition of phases and of the whole rock considered in this study (*shaded region*) after projection from albite. Apices are *A*: Al_2O_3, *F*: FeO; *M*: MgO, projected from K_2O (considered to perfectly mobile) albite, quartz and vapour (in excess)

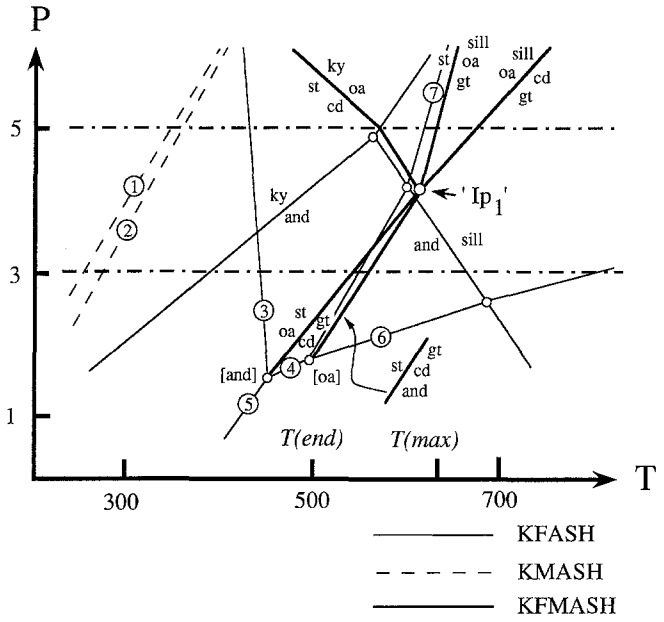

Fig. 3. P-T grid showing univariant and divariant reactions in the system FMASH and the position of the aluminosilicate stability fields (calculated from Powell and Holland's "THERMOCALC" 1990). Reactions: *1* (sill) mg−oa+mg−st=mg−cd, *2* (mg−oa) mg−st=mg−cd+sill, *3* (py) fe−st+fe−oa=alm, *4* (fe−oa) fe−st+alm=fe−cd, *5* (alm) fe−st+fe−oa=fe−cd, *6* (fe−st) alm+and=fe−cd, *7* (fe−oa) fe−st=alm+sill. *T(end)* and *T(max)* refer to the lower and upper bounds on the range in temperatures during which cordierite-orthoamphibole parageneses could develop at Springton (see Fig. 8)

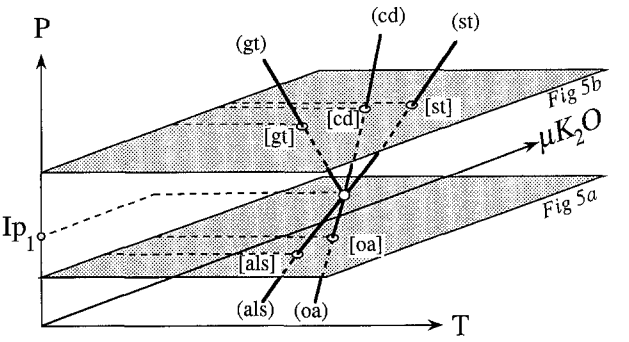

Fig. 4. Univariant lines in KNFMASH are, in reality, lines in P-T-μ space. However, when represented in μ-T or μ-P space the arrangement of points and lines we see are the projections onto a plane (μ-T or μ-P) of the whole system. Lines in P-T-μ space become points intersecting a plane, planes are projected as lines and volumes appear as fields in μ-T or μ-T space. This figure shows schematically the disposition for univariants around Ip_1 in P-T-μK_2O space and their intersection with T-μK_2O planes at $P<Ip_1$ (Fig. 5a) and $P>Ip_1$ (Fig. 5b)

of the invariant point in NFMASH system will occur at lower pressure and temperature than the FMASH invariant point, along the metastable part of the [oa] absent univariant line, expanding the orthoamphibole field with respect to other minerals.

Table 1. Mineral compositions used for calculating reactions in the system KNFMASH, slightly modified from natural compositions in the Springton cordierite-orthoamphibole samples 911-048 and 911-107; see Table 2). Note that following Schumacher and Robinson (1987) we have assumed hydrated cordierite

	$NaO_{0.5}$	FeO	MgO	$AlO_{1.5}$	SiO_2	$HO_{0.5}$	$KO_{0.5}$
oa	0.66	3.56	2.00	3.37	6.00	2.00	0.00
cd	0.00	0.70	1.30	4.00	5.00	0.75	0.00
st	0.00	3.50	0.80	18.0	7.20	4.00	0.00
bt	0.00	1.30	1.20	1.60	2.80	2.00	0.90
q	0.00	0.00	0.00	0.00	1.00	0.00	0.00
als	0.00	0.00	0.00	2.00	1.00	0.00	0.00
g	0.00	2.58	0.42	2.00	3.00	0.00	0.00
ab	1.00	0.00	0.00	1.00	3.00	0.00	0.00

KNFMASH with variable μK_2O

The phases considered so far have only a very small capacity to accommodate K_2O and thus the addition of only small amounts of K_2O must stabilize biotite. In KNFMASH assemblages the addition of biotite to the NFMASH univariant assemblages will necessarily buffer the μK_2O at any given P or T. Consequently univariant lines in KNFMASH appear as pseudo-invariant points in isobaric μK_2O-T (or isothermal μK_2O-P) space; that is they form "piercing points" in any plane in μK_2O-T-P space (see Fig. 4). In μK_2O-T space there are two fundamentally different topologies, sections at $P>Ip_1$ involving the pseudo-invariants [gt], [st] and [cd] or sections at $P<Ip_1$ involving the pseudo-invariants [als] and [oa] (see Fig. 3).

μK_2O-T sections can be constructed provided the appropriate thermodynamic data are available. Importantly, however, μK_2O-T sections are topologically equivalent to μK_2O–($-\mu H_2O$) diagrams, which can be constructed entirely on the basis of the reaction coefficients using mineral compositions from natural assemblages (Ferry and Burt 1982). The compositions of the phases used here are given in Table 1 and are based on natural compositions from cordierite-orthoamphibole rocks in the Springton area (see next section). The slopes of pseudo-invariant lines calculated from reaction coefficients have been used to constrain the relative positions of KNFMASH, KNMASH and KNFASH reaction lines and pseudo-invariant points in μK_2O-"T"-space (Fig. 5) (note that the slopes of the univariants have been slightly distorted for the sake of clarity).

KNFMASH pseudo-sections for constant X_{Fe} bulk compositions

The positions of univariant (or discontinuous) reaction curves in the KNFMASH system are necessarily fixed in intensive variable (P-T-μ) space, independent of the composition. In contrast, the positions of continuous reactions, which are generally far more important in the formation of new minerals and their textural development, are dependent on the bulk composition of a rock, particularly the X_{Fe} (e.g. Hensen 1971). To interpret the textural development and reaction history in natural

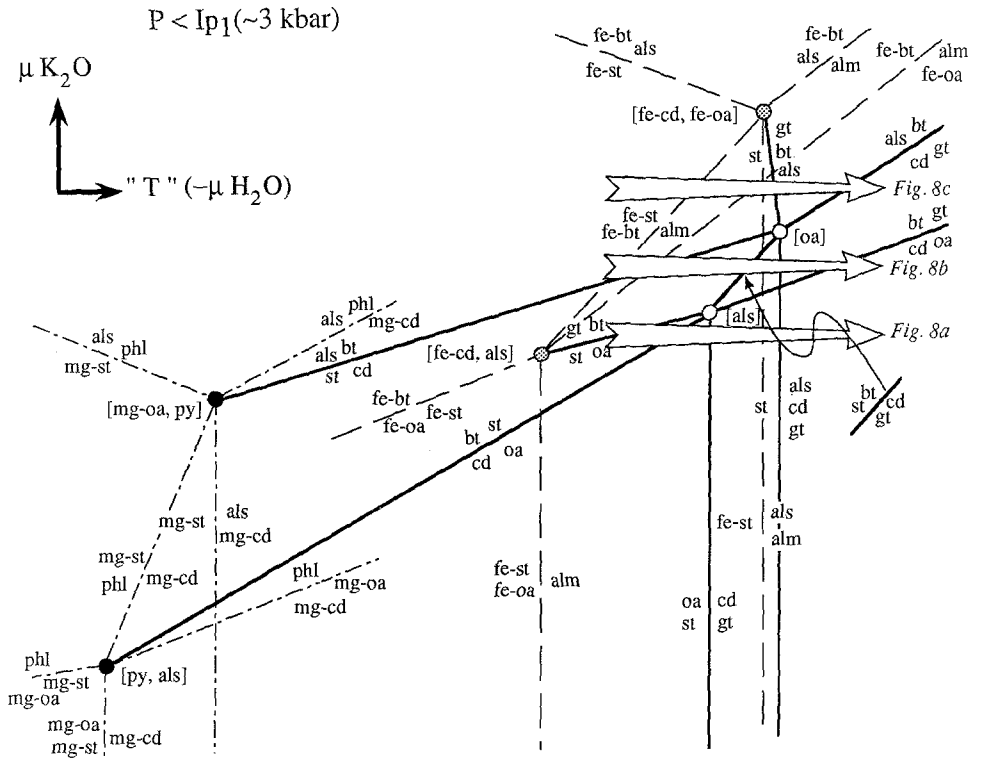

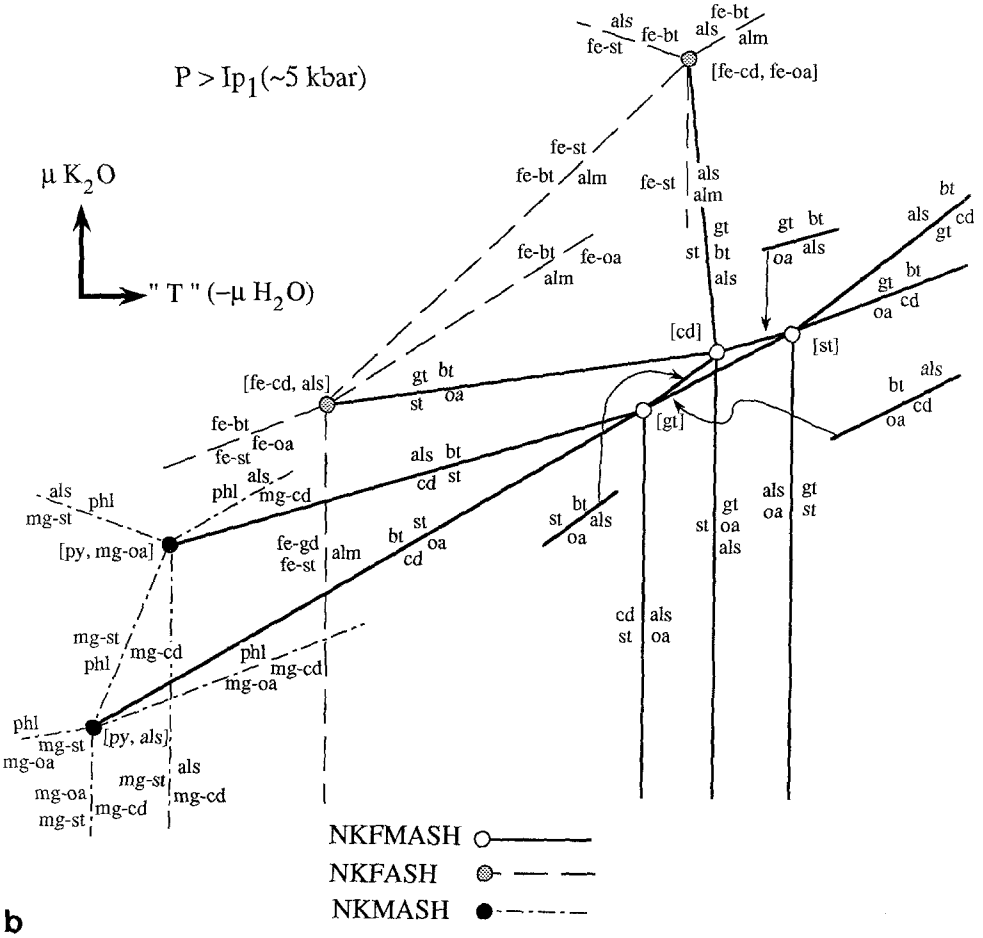

Fig. 5a, b. $\mu K_2O - T$ diagrams showing pseudo-invariant points and pseudo-univariant lines in KNFMASH, KNFASH and KNMASH; **a** for $P < Ip_1$; **b** for $P > Ip_1$

rocks, it is therefore useful to construct diagrams in intensive variable space that explicitly show the position of the divariant or continuous reaction fields for a given bulk composition. The great majority of continuous reactions are dictated by the changing X_{Fe} of coexisting Fe–Mg minerals, so here schematic diagrams appropriate to a range of X_{Fe} for Fe-rich to Mg-rich compositions (pseudo-sections) are constructed. Figures 6 and 7 illustrate the pseudosection for varying X_{Fe} at $P < Ip_1$ and $P > Ip_1$ (~3 kbar and 5 kbar), respectively. Arrows indicate the direction along univariants in which compositions of the phases become progressively more magnesian. Figures 6 and 7 demonstrate that with changing X_{Fe} the sequence of reactions encountered by the same path in μK_2O-"T" space varies dramatically. For both Fe-rich and Mg-rich compositions, the phase relationships in $P < Ip_1$ and $P > Ip_1$ are similar (e.g. Figs. 6b, 7b). However, the difference between the sections is obvious at intermediate compositions where the trivariant assemblage oa+als occurs for $P > Ip_1$, but is absent for $P < Ip_1$. The relative complexity of pseudo-sections for $P > Ip_1$ compared to those for $P < Ip_1$ is due to the triangular arrangement of KNFMASH pseudo-univariants around the three pseudo-invariants stable at that pressure.

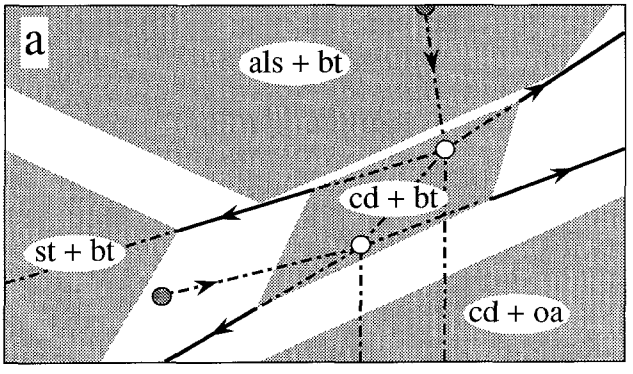

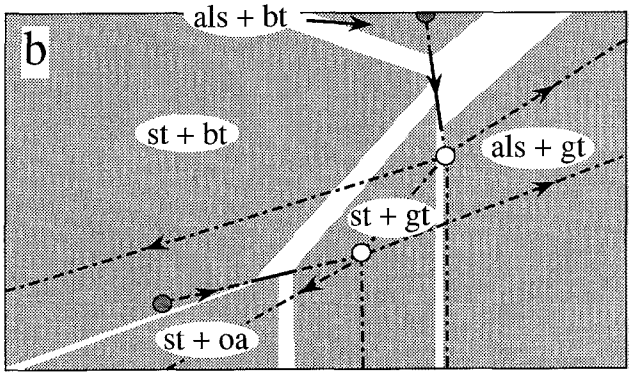

Fig. 6a, b. KNFMASH pseudo-sections for varying bulk compositions at $P < Ip_1$ for the central part of the T-μK_2O space shown in Fig. 5a. **a** Constructed for intermediate X_{Fe} compositions, while **b** is for high X_{Fe} compositions. *Stippled regions* show pseudo-trivariant fields separated by pseudo-divariant fields. *Solid lines* indicate univariant reactions seen by a rock of specific bulk composition; *dashed lines* indicate univariant reactions which are not seen. *Arrows* indicate the direction along univariants in which compositions of the phases become progressively more magnesian

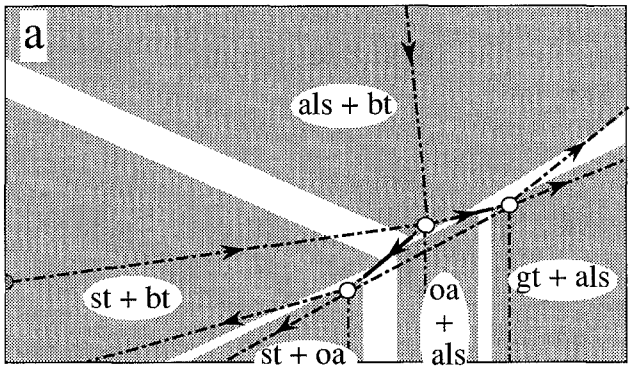

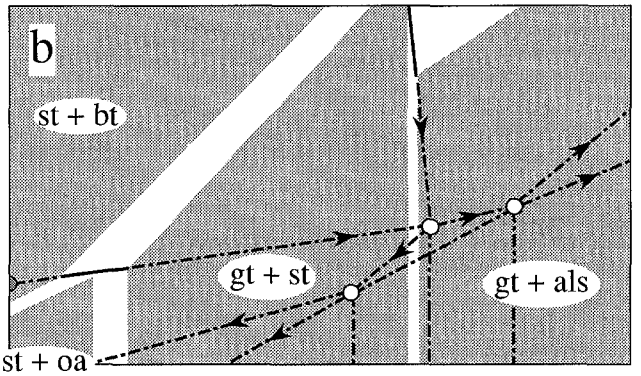

Fig. 7a, b. KNFMASH pseudo-sections for varying bulk compositions at $P > Ip_1$ for the central part of the T-μK_2O space shown in Fig. 5b. **a** Constructed for intermediate X_{Fe} compositions, while **b** is for high X_{Fe} compositions. *Stippled regions* show pseudo-trivariant fields separated by pseudo-divariant fields. *Solid lines* indicate univariant reactions seen by a rock of specific bulk composition; *dashed lines* indicate univariant reactions which are not seen. *Arrows* indicate the direction along univariants in which compositions of the phases become progressively more magnesian

$\mu FeMg_{-1}$–(μK_2O-"T") space

While Figs. 6 and 7 show the gross detail of the reaction space for a specific X_{Fe} bulk composition is it also useful to construct diagrams, which enable comparison of the reaction history of rocks with different X_{Fe} travelling along an otherwise similar path through intensive variable space. For a given path in μK_2O-"T" space, the sequence of continuous and discontinuous reactions encountered by different X_{Fe} bulk compositions can be readily portrayed in $\mu FeMg_{-1}$–(μK_2O-"T") space (e.g. Schumacher and Robinson 1987). Figure 8 shows the $\mu FeMg_{-1}$–(μK_2O-"T") space appropriate to three μK_2O-"T" paths indicated by the arrows in Fig. 5a.

The schematic μK_2O-"T" diagrams (Figs. 6–8) provide the basis for evaluating textures developed in semipelites in response to high temperature metasomatic depletion of K_2O and, as such, can be applied to cordierite-orthoamphibole rocks from a wide range of localities for varying physical conditions. In the following section we use these diagrams to interpret the reaction history of the cordierite-orthoamphibole rocks from the Springton region, South Australia.

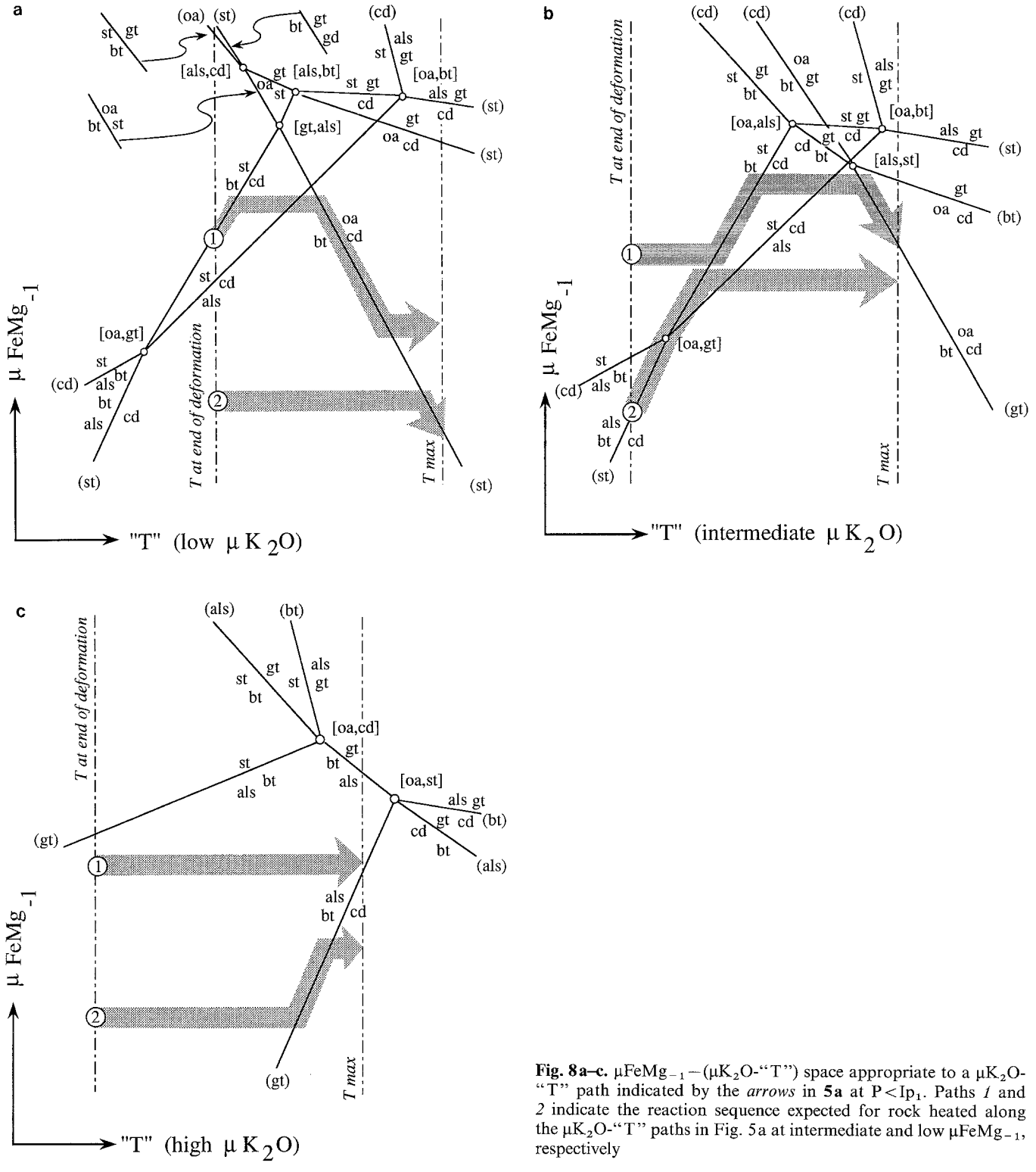

Fig. 8a–c. $\mu FeMg_{-1}-(\mu K_2O$-"T") space appropriate to a μK_2O-"T" path indicated by the *arrows* in **5a** at $P<Ip_1$. Paths *1* and *2* indicate the reaction sequence expected for rock heated along the μK_2O-"T" paths in Fig. 5a at intermediate and low $\mu FeMg_{-1}$, respectively

Cordierite-orthoamphibole rocks in the Springton region

Cordierite-orthoamphibole rocks of presumed Cambrian age occur in the Kanmantoo Group on the eastern edge of the Mount Lofty Ranges in an area between the towns of Springton and Cambrai, approximately 60 km ENE of Adelaide in South Australia (Sandiford et al. 1990). The Kanmantoo Group forms the youngest sedimentary sequence of the early Palaeozoic Southern Adelaide Fold-belt. In the Springton region the Kanmantoo Group consists mainly of immature psammites and semi-pelites with rare pelites, limestones and calc-silicates intruded by subconcordant granite veins. Porphyroblastic cordierite-orthoamphibole rocks occur as isolated pods ranging in size from 2 to 100 m in length within the psammite, semi-pelite sequence. The macroscopic outcrop pattern as revealed by an almost continuous layer of impure limestone indicates a relatively simple structure dominated by a north-south trending upright, tight synform (Sandiford et al. 1990). The strong foliation, axial to the synform, is defined by the alignment of biotites.

Petrography

The cordierite-orthoamphibole rocks consist predominantly of a strongly foliated quartz-biotite matrix with lesser plagioclase, tourmaline, apatite, zircon, opaques, including magnetite and ilmenite, phosphate minerals (monazite and xenotime), and porphyroblasts of orthoamphibole and cordierite. Staurolite and andalusite and, in one recorded case, garnet also occur. Potassium-feldspar and muscovite do not occur as prograde phases in cordierite-orthoamphibole rocks but do so in the adjacent pelites. Chlorite, rutile and muscovite are observed as retrograde minerals.

Cordierite porphyroblasts are often seamed with slightly curved inclusion trails which can be traced into the matrix foliation (type 1 cordierite, Fig. 10), but also occur with relatively few randomly oriented inclusions (type 2 cordierite, Figs. 12–14). Type 2 cordierite is typically associated with orthoamphibole which occurs as stellar aggregates cross-cutting the biotite fabric (Fig. 11). The proportions of biotite and orthoamphibole existing in close proximity are inversely related, suggesting the formation of orthoamphibole at the expense of biotite. Staurolite porphyroblasts exhibit spectacular inclusion trails (Fig. 12), similar to those in type 1 cordierite porphyroblasts, which indicate syn-deformational porphyroblast growth. In cordierite-orthoamphibole bearing rocks staurolite is always rimmed by type 2 cordierite (Fig. 12, cf. Fig. 9). Prismatic sillimanite and andalusite both occur as inclusions in type 2 cordierite (Fig. 13) which always physically separates them from orthoamphibole. Garnet has been observed in only one cordierite-orthoamphibole bearing rock, as a porphyroblast sieved with xenotime inclusions replacing cordierite (Fig. 14).

The two varieties of cordierite reflect two distinct phases of cordierite growth. Type 1 cordierite growth occurred during the deformation which gave rise to the biotite foliation, while type 2 occurred after deformation ceased. The similarity in morphology of the inclusion trails in staurolite and type 1 cordierite suggest formation at a similar stage of deformation and metamorphism (Fig. 15) while the presence of staurolite as relict inclusions in moats of type 2 cordierite implies the breakdown of staurolite after deformation ceased. Randomly oriented orthoamphibole associated with type 2 cordierite and in inverse proportion to biotite suggests that cordierite and orthoamphibole are an equilibrium assemblage, the formation of which involves the consumption of biotite. In summary the textural development of cordierite-orthoamphibole rocks suggests syn-deformation growth of st−bt−plag−q± Type 1 cd, and, and−bt−plag−q±Type 1 cd assemblages, with subsequent (post-deformation) breakdown of st+bt and and+bt to Type 2 cd+oa (Fig. 15).

In contrast with cordierite-orthoamphibole rocks, the pelitic rocks contain either muscovite or K-feldspar as a prograde phase in addition to biotite and aluminosilicate. Andalusite and staurolite occur as poikiloblasts, up to 12 mm across, with inclusion trails which are straight or occasionally crenulated (Fig. 9). Andalusite is frequently associated with prismatic sillimanite. Early formation

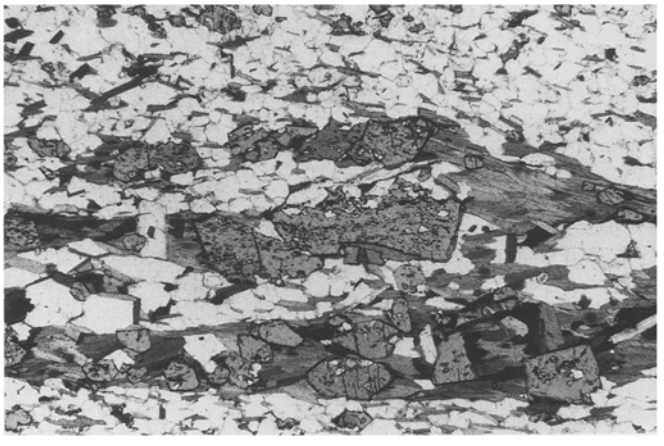

Fig. 9. Staurolite biotite pelitic schist from the Springton region. Note inclusion trails in staurolites (cf. Fig. 12). Width of view is 24 mm

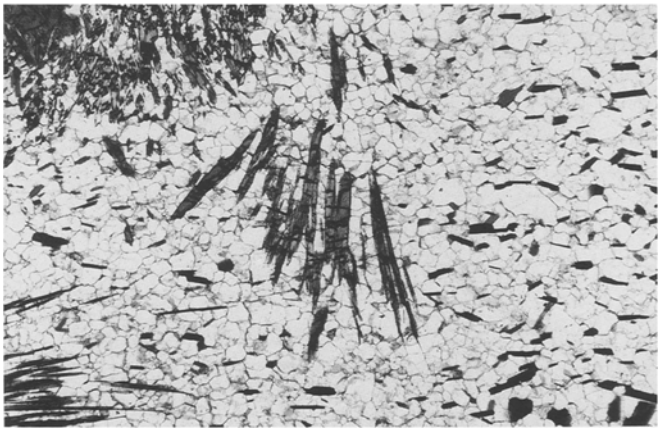

Fig. 11. Splays of orthoamphibole crystals cross-cutting the biotite fabric. Width of view is 24 mm

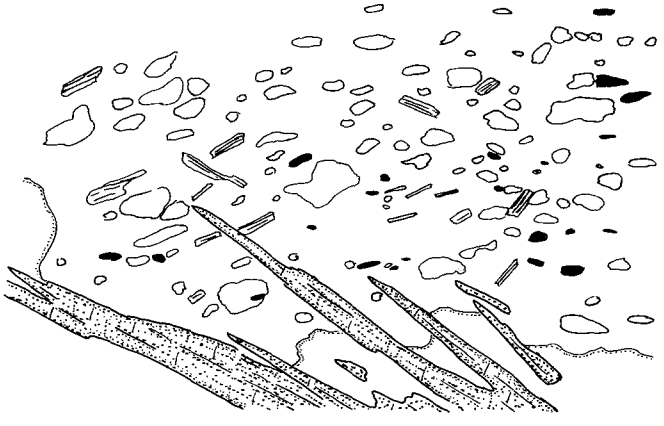

Fig. 10. Type 1 cordierite poikiloblasts with biotite quartz inclusion trails (*top right*) and biotite-quartz feldspar fabric (*bottom left*) cross-cut by orthoamphibole prisms. Width of view is 6 mm

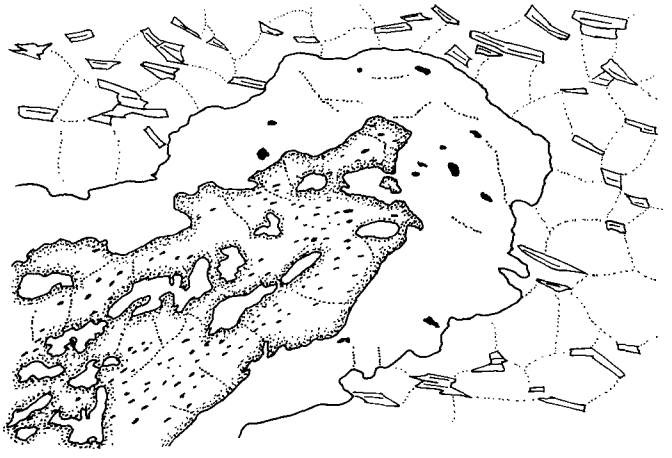

Fig. 12. Staurolite with curved inclusion trails of quartz and ilmenite, rimmed by type 2 cordierite. Width of view is 24 mm

Fig. 13. Andalusite (*stippled*) and sillimanite (*diamond-shaped* sections) separated from biotite-quartz-plagioclase matrix by type 2 cordierite (+ilmenite). Width of view is 6 mm

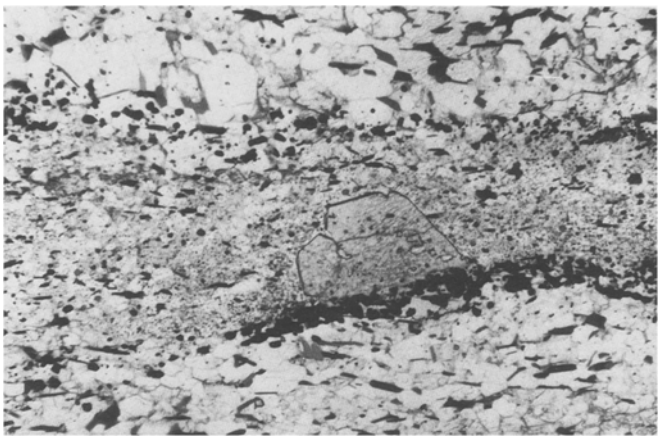

Fig. 14. Garnet replacing type 2 cordierite. Width of view is 24 mm

of andalusite is implied by crenulated inclusion trails while prismatic sillimanite cross-cuts the biotite fabric, indicating a transition from the andalusite stability field to that of sillimanite after deformation had ceased. Fibrolitic sillimanite occurs commonly growing over the biotite foliation. Quartz segregations several kilometres from the cordierite-orthoamphibole rocks contain all three Al_2SiO_5 polymorphs (Sandiford et al. 1990) with textural evidence for the replacement of early formed kyanite by andalusite and subsequently by sillimanite.

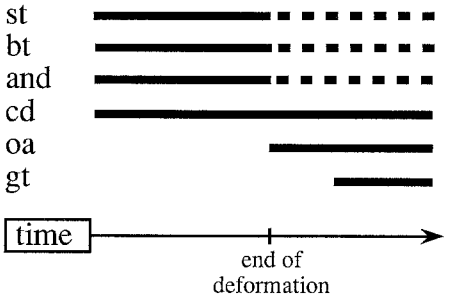

Fig. 15. Summary of mineral growth sequence in Springton cordierite-orthoamphibole rocks. *Solid lines* indicate mineral growth; *dashed lines* indicate consumption

Mineral chemistry

Selected electron microprobe compositional data for orthoamphibole, cordierite, staurolite, biotite, plagioclase, and garnet are given in Table 2. The X_{Fe} of orthoamphiboles is in the range 0.44–0.68, while the composition is generally that of gedrite, related to anthophyllite by 0.59–0.68 edenite ($Na_1Al_1Si_{-1}v_{-1}$) and 1.44–1.65 tschermakite ($Al_2Si_{-1}Mg_{-1}$) substitutions per unit formula. Orthoamphibole in andalusite-bearing rocks from the Springton region has less edenite and tschermakite substitution (0.33 and 0.60 respectively). Staurolite X_{Fe} is in the range 0.80–0.85, while EDS analyses indicate, qualitatively, a small amount of Zn. Biotite has a wide range of X_{Fe} (0.26–0.55), depending on the phases with which it co-exists. The composition of biotite can be related to phlogopite by 0.22–0.42 tschermakite ($Al_2Si_{-1}Mg_{-1}$) and 0.61–1.34 $FeMg_{-1}$ substitutions

Table 2. Selected electron microprobe analyses of silicate assemblages in cordierite-orthoamphibole rocks from Springton. Sample 185/413 contains primary andalusite

Sample	911/048					911/107				185/413		
Phase	oa	cd	st	bt	plag	oa	cd	gt	bt	oa	cd	bt
SiO_2	39.64	48.82	25.55	36.32	69.35	38.68	47.69	36.53	35.34	49.37	49.02	38.30
TiO_2	0.22	0.00	0.48	1.28	0.00	0.00	0.00	0.00	1.52	0.21	0.00	1.32
Al_2O_3	18.55	34.08	54.61	17.84	21.34	18.67	33.31	20.90	17.93	7.05	34.40	17.51
FeO	28.31	8.37	15.09	19.94	0.17	28.59	8.51	37.33	20.86	23.25	6.30	15.01
MnO	0.28	0.00	0.00	0.00	0.00	0.32	0.00	1.45	0.00	0.35	0.00	0.00
MgO	8.67	8.74	1.96	10.93	0.00	7.62	8.09	3.38	9.67	15.78	10.13	14.41
CaO	0.00	0.00	0.46	0.00	0.32	0.00	0.00	0.18	0.00	0.00	0.00	0.00
Na_2O	2.15	0.50	0.00	0.42	11.16	2.27	0.59	0.00	0.53	1.02	0.52	0.49
K_2O	0.00	0.00	0.00	8.91	0.08	0.00	0.00	0.00	8.72	0.00	0.00	8.76
Total	97.9	100.5	98.2	95.6	102.4	96.2	98.2	99.8	94.6	97.1	100.4	95.8
X_{Fe}	0.65	0.35	0.81	0.51	—	0.68	0.37	0.86	0.55	0.45	0.26	0.37

Table 3. X_{Fe} of biotites in various pelitic and semi-pelitic assemblages (including cordierite-orthoamphibole assemblages) from the Springton Region

Assemblage	X_{Fe} of bt
gt	0.53–0.54
st + cd	0.51–0.58
als	0.46–0.52
als + cd	0.38–0.47
cd	0.26–0.39

per unit formula. Importantly, the ratio Al:(Fe+Mg) in biotite is marginally less than coexisting garnet and greater than orthoamphibole when projected from albite (see Fig. 2). Garnet is Fe-rich, comprising 83% almandine and 13% pyrope and has very small spessartine and grossular components, with $X_{Fe}=0.86$. Plagioclase is sodic, with compositions in the range $An_{3-21}Ab_{79-97}$.

The composition of biotite in rocks from the Springton region enables the comparison of the X_{Fe} of biotites in the various assemblages (Table 3). Biotites associated with garnet have the most Fe-rich compositions, closely followed by those containing staurolite plus cordierite, then aluminosilicate-bearing rocks. Andalusite plus cordierite assemblages have lower X_{Fe} biotites, while those in cordierite-only rocks are the most Mg-rich. Sample 911-123 contains staurolite, cordierite and biotite all with anomalously high X_{Fe} (i.e. $X_{Fe,bt}=0.58$). This is probably due to a higher than usual oxidation state, as evidenced by its association with magnetite. In summary, X_{Fe} decreases in the order gt > st > oa > bt > cd, while the ratio of Al to (Fe+Mg) when projected form albite decreases in the order als > st > cd > gt > bt > oa.

Physical conditions of metamorphism

Pressure and temperature conditions for the Kanmantoo Group in the Springton region have been calculated by Sandiford et al. (1990). Using the Holland and Powell (1985) data set, they established a range of 530–680° C and 3–5 kbars for the region. The compositions of gt – bt pairs yield temperatures in the range 590–610° C (Ferry and Spear 1978). Textural evidence cited by Sandiford et al. (1990) for the transition from kyanite to andalusite then sillimanite stability fields suggests an essentially isobaric heating path at pressures below the aluminosilicate triple point. Sandiford et al. (1990) argued that the distribution of assemblages in pelites in the Springton region implied much of the sequence is internally buffered with respect to fluid composition. In the neighbourhood of the cordierite-orthoamphibole rocks considered here internal buffering of fluid compositions is suggested by the occurrence of both sillimanite – K-feldspar – quartz and muscovite – quartz equilibrium assemblages in the pelites, which imply variations in a_{H_2O} (Kerrick 1972).

Reaction textures in cordierite-gedrite rocks from Springton

The textures in cordierite-gedrite rocks from the Springton region indicate that the consumption of staurolite and/or andalusite was an important step in the stabilization of the cordierite-orthoamphibole assemblage. Since this breakdown of aluminosilicate or staurolite to cordierite and orthoamphibole cannot result from a "closed system" divariant reaction in NFMASH the reaction must involve an additional phase or open system behaviour or a combination of both. The textures suggest the involvement in the reaction of biotite and since no product phases contain K_2O, the reactions cannot conserve K_2O, e.g.

(gt, als) $st + bt + q + ab = gd + cd + H_2O + K_2O$
(gt, st) $als + bt + q + ab = gd + cd + H_2O + K_2O$

Together with the textural evidence for essentially isobaric heating of the sequence (see Sandiford et al. 1990) this indicates that the appropriate way to understand the reaction history of the Springton cordierite-orthoamphibole rocks is with reference to μK_2O-"T" space (e.g. Figs. 6–8).

The pressures at which metamorphism occurred (3–5 kbars) are sufficiently uncertain that is is not possible to decide independently on the applicability of the two alternative μK_2O-"T" topologies shown in Fig. 5, i.e. at $P < Ip_1$ or at $P > Ip_1$. However, the absence in the Springton region of rocks containing the stable assemblage aluminosilicate-orthoamphibole suggests that the diagram at $P > Ip_1$ is invalid for this area, leaving Fig. 5a (and related figures constructed for $P < Ip_1$) as the appropriate alternative. At the end of foliation development four distinct assemblages can be recognised in the rocks which subsequently reacted to produce type 2 cordierite and orthoamphibole. In order of decreasing $X_{Fe,bt}$ (Table 2) the four "starting" assemblages are st + bt, st + cd + bt, cd + bt, and + bt. We assume that metasomatism of these rocks occurred in response to passage of fluids (for justification see finalsection) the composition of which was controlled by an external reservoir. The composition of the fluid phase is therefore assumed constant and since the close proximity of the different assemblages precludes different P-T histories, all variations in the reaction history are attributed to variations in μK_2O or X_{Fe} or a combination of the two. The mineral analyses summarised in Table 2 show that there are substantial differences in the $X_{Fe,bt}$ of the different "starting" assemblages and thus much of the variation in the reaction history of these different assemblages is attributable to X_{Fe}. However, assuming that these "starting" assemblages equilibrated at identical P-T conditions (i.e. those that prevailed at the end of the foliation development), then at least some of the variation must be due to differences in μK_2O. For example, Fig. 8 shows that als – cd – bt and st – cd – bt assemblages can only occur at the same T at different μK_2O, independent of relative X_{Fe}. Specifically, als – cd – bt (e.g. Path 2 in Fig. 8b) will occur in rocks of higher μK_2O than st – cd – bt (e.g. Path 1 in Fig. 8a).

Implications for metamorphism at Springton

An important question in metamorphic geology concerns the distribution and behaviour of the fluids that must be generated as a consequence of prograde metamorphism of sediments. Of particular concern is the effect of these fluids on the distribution of heat and matter within the terrain. We have shown that cordierite-orthoamphibole rocks are to be expected during metasomatic depletion of K_2O from the semi-pelites at medium grades of metamorphism. At Springton the textural evidence for the formation of cordierite and orthoamphibole at the expense of staurolite or andalusite and biotite implies a reaction which releases K_2O. Cordierite-orthoamphibole rocks form pods up to 100 m in length in the semi-pelites and the transport distances of K_2O during metasomatism are necessarily of the same or greater order. Since diffusion distances for most species within stationary fluids on the timescale of orogenic events are, at best, of the order of 0.1–1 m and the diffusion rates of components through solid phases are significantly slower (Carmichael 1969) it is likely that an advecting fluid provided the vector enabling metasomatism. Additional evidence for locally significant fluid advection in the Springton region comes from work by M. Sandiford and P. Dymoke (in preparation) which shows large, but heterogeneous, shifts in $\delta^{18}O$ of calcites in marbles interlayered with the clastic sequence, from $\delta^{18}O \sim +23$ to as low as $\delta^{18}O \sim +13‰$.

The interpretation that high temperature metasomatic formation of cordierite-orthoamphibole rocks is a consequence of fluid transport implies that the distribution of advecting fluids during metamorphism must be reflected, in part, in the outcrop pattern of the metasomatised rocks. The plan form of cordierite-orthoamphibole rocks, reflected in their pod-like distribution, suggests that fluid movement was along pipe- or chimney-like columnar paths. In contrast with the cordierite-orthoamphibole rocks, in which the fluid composition was likely to have been externally buffered, the adjacent pelites, which variously contain muscovite-quartz and K-feldspar-sillimanite as prograde phases, imply internal buffering, therefore precluding pervasive fluid infiltration. Rather, the advecting fluids must have moved only through parts of the terrain. The movement of fluids through a metamorphic terrain may have a substantial effect on the thermal structure of the terrain if large fluid-rock ratios are involved (e.g. Connolly and Thompson 1989). In the Springton region it appears that only relatively small areas have been affected by the passage of fluids, and that the thermal effects, if any, of fluid advection are thus confined to very small regions. It seems unlikely, therefore, that advecting fluids responsible for the generation of cordierite-orthoamphibole rocks at Springton have had any significant effect on the thermal structure of the terrain as a whole.

References

Baker J, Powell R, Sandiford M, Muhling J (1987) Corona textures between kyanite, garnet and gedrite in gneisses from Errabiddy, Western Australia. J Metamorph Geol 5:357–370

Carmichael DM (1969) On the mechanism of prograde metamorphic reaction in quartz-bearing pelitic rocks. Contrib Mineral Petrol 20:244–267

Chinner GA, Fox JS (1974) The origin of cordierite-anthophyllite rocks in the Land's End aureole. Geol Mag 111:397–408

Connolly JAD, Thompson AB (1989) Fluid and enthalpy production during regional metamorphism. Contrib Mineral Petrol 102:349–366

Ferry JM, Burt DM (1982) Characterization of metamorphic fluid composition through mineral equilibria. In: Ferry JM (ed) Characterisation of metamorphism through mineral equilibria. (Reviews in Mineralogy, vol 10). Mineralogical Society of America, Chelsea, Michigan, pp 207–262

Ferry JM, Spear FS (1978) Experimental calibration of the partitioning of Fe and Mg between biotite and garnet. Contrib Mineral Petrol 66:13–117

Harley SL (1985) Paragenetic and mineral-chemical relationships in orthoamphibole-bearing gneisses from Enderby Land, Eastern Antarctica: a record of Proterozoic uplift. J Metamorph Geol 3:179–200

Hensen HJ (1971) Theoretical phase relations involving cordierite and garnet in the system $MgO-FeO-Al_2O_3-SiO_2$. Contrib Mineral Petrol 33:191–214

Holland TJB, Powell R (1985) An internally consistent thermodynamic dataset with uncertainties and correlations: 2. Data and results. J Metamorph Geol 3:343–370

Holland TJB, Powell R (1990) An enlarged and updated internally consistent data set with uncertainties and correlations: the system $K_2O-Na_2O-CaO-MgO-MnO-Fe_2O_3-Al_2O_3-TiO_2-SiO_2-C-H_2-O_2$. J Metamorph Geol 8:89–124

Hudson NFC, Harte B (1985) K_2O-poor aluminous assemblages from the Buchan Dalradian, and the variety of orthoamphibole assemblages in aluminous bulk compositions in the amphibolite facies. Am J Sci 285:224–266

Kerrick DM (1972) Experimental determination of muscovite and quartz stability with $P_{H_2O} < P_{total}$. Am J Sci 272:946–958

Powell R, Holland TJB (1988) An internally consistent dataset with uncertainties and correlations: 3. Applications to geobarometry, worked examples and a computer program. J Metamorph Geol 6:173–204

Robinson P, Jaffe HW (1969) Aluminous enclaves in gedrite-cordierite gneiss from south-western New Hamsphire. Am J Sci 267:389–421

Sandiford M, Oliver RL, Mills KJ, Allen RVA (1990) A cordierite-staurolite-muscovite association, east of Springton, Mt Lofty Ranges: implications for the metamorphic evolution of the Kanmantoo Group (Special Publication no. 16). Geological Society of Australia, Brisbane, Australia, pp 483–494

Schumacher JC, Robinson P (1987) Mineral chemistry and metasomatic growth of aluminous enclaves in gedrite-cordierite-gneiss from southwestern New Hampshire, USA. J Petrol 28:1033–1073

Sharma RS, MacRae ND (1981) Paragenetic relations in gedrite-cordierite-staurolite-biotite-sillimanite-kyanite gneisses at Ajitpura, Rajasthan, India. Contrib Mineral Petrol 78:48–60

Spear FS, Schumacher JC (1982) Orthoamphibole and cummingtonite amphibolites. In: Veblen DR, Ribbe PH (eds) Amphiboles: petrology and experimental phase relations (Reviews in Mineralogy, vol 9B) Mineralogical Society of America, Chelsea, Michigan, pp 159–182

Editorial responsibility: R. Binns